Eur. Phys. J. A **18**, 377–381 (2003)
DOI 10.1140/epja/i2002-10240-4

THE EUROPEAN PHYSICAL JOURNAL A

The (spin) structure of the nucleon

G. van der Steenhoven[a]

For the HERMES Collaboration
Nationaal Instituut voor Kernfysica en Hoge-Energiefysica (NIKHEF), P.O. Box 41882, 1009 DB Amsterdam, The Netherlands

Received: 30 September 2002 /
Published online: 22 October 2003 –

Abstract. A selection of new data obtained by the HERMES experiment at DESY is presented, which provides new insight into the QCD structure of the nucleon. Using polarized lepton beams and polarized targets, the spin-dependent structure function $g_1(x)$ has been determined for ^{1}H, ^{2}H and ^{3}He. By also observing one of the produced hadrons it has been possible to extract the polarization distribution of individual quark flavours in the nucleon as well. Further information on nucleon structure has been obtained by observing (almost) exclusive reactions, which can be interpreted in terms of the recently introduced generalized parton distributions (GPDs). As an example of such data measurements of both the beam-spin and beam-charge asymmetries resulting from deeply virtual Compton scattering (DVCS) are presented. By embedding the deep-inelastic scattering process in the nuclear environment additional information can be obtained on nucleon structure and some QCD effects. The potential of this technique is illustrated by showing new results on tagged structure functions and hadronization in nuclei.

PACS. 13.60.Hb Total and inclusive cross-sections (including deep-inelastic processes) – 13.88.+e Polarization in interactions and scattering – 14.20.Dh Protons and neutrons – 24.85.+p Quarks, gluons, and QCD in nuclei and nuclear processes

1 Introduction

Studies of the QCD structure of the nucleon are entering a new phase because of a wealth of new measurements that recently has come available, and because of some recent theoretical developments. Two examples are mentioned. Experimentally, new data on the longitudinal spin-structure of the nucleon enable a precise determination of the flavour-separated quark polarization distributions in the nucleon. Theoretically, the introduction of generalized parton distributions provides a new unified framework to access dynamic correlations between partons in the nucleon on the basis of various —quite different— reactions.

Moreover, progress is also reported from more familiar areas of research such as studies of the effect of the nuclear medium on deep-inelastic scattering. The renewed interest in this domain is exemplified by the claim that energy-loss measurements based on semi-inclusive deep-inelastic scattering data on nuclei can be linked to energy loss phenomena in relativistic heavy-ion collisions [1]. Furthermore, first data on recoil detection in deep-inelastic scattering have created considerable interest as well.

In this paper many of these developments are summarized with emphasis on those subjects where recent HERMES data are available. The paper is organized as follows. In the next section new results on the spin structure of the nucleon are presented. Subsequently, in sect. 3 the subject of Generalized Parton Distributions is discussed. The fourth section is devoted to nuclear effects, while the paper is concluded in the last section.

[a] e-mail: gerard@nikhef.nl

2 The spin structure of the nucleon

So far most of the experimental effort in the field of spin physics has been dedicated to precise measurements of the inclusive spin-dependent structure function $g_1(x)$. In subsect. 2.1 the presently available data on $g_1(x)$ are reviewed. In recent years, both SMC and HERMES have been able to decompose the quark spin distribution into several distinct distributions for each quark flavour [2,3] including a determination of the flavour dependence of the sea-quark spins. These data are presented in subsect. 2.2.

2.1 The spin structure function $g_1(x)$

The polarized structure function $g_1(x)$ contains information on the helicity-dependent quark contribution to the deep-inelastic scattering cross-section. The available data on $g_1(x)$ on the proton [4–7] are displayed in the top

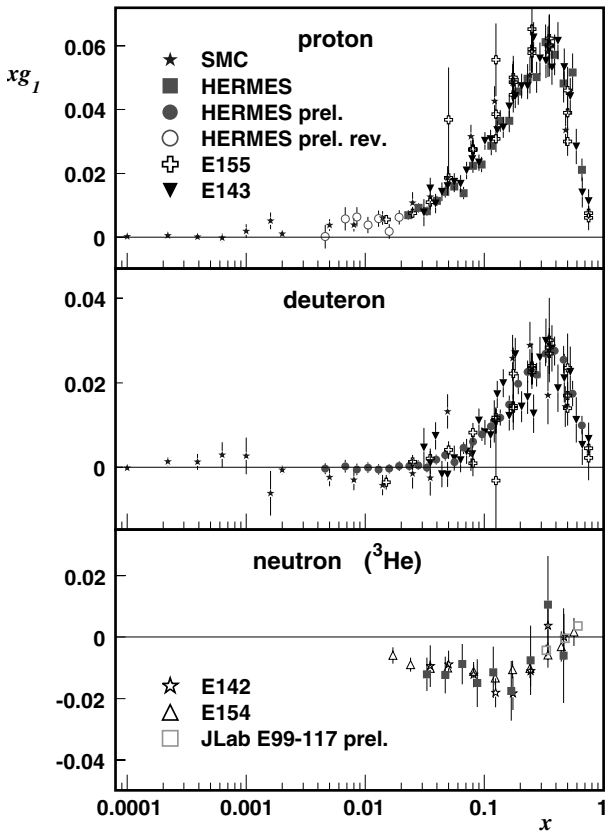

Fig. 1. The longitudinal spin-dependent structure function $g_1(x)$ (mutiplied by x) as measured on longitudinally polarized hydrogen (top panel), deuterium (middle panel) and ^{3}He (lower panel) targets. All data are shown at the *measured* Q^2 values.

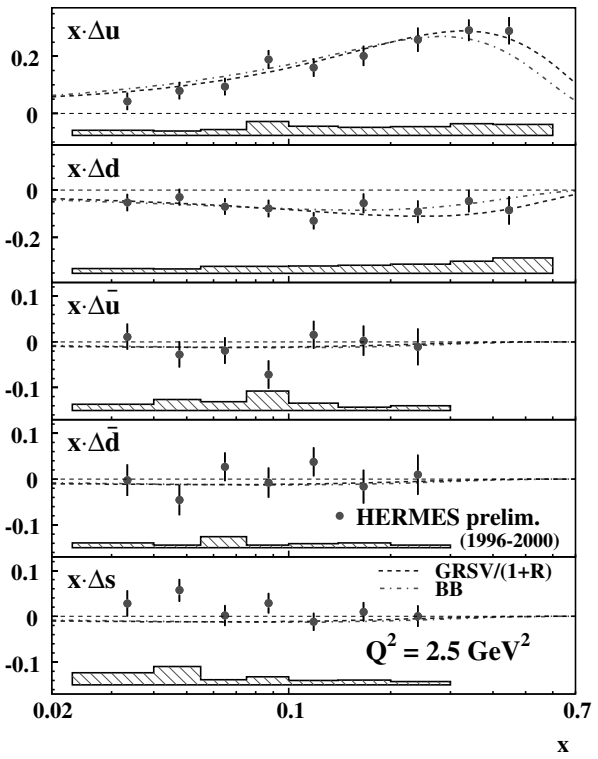

Fig. 2. The x-weighted longitudinal quark spin distribution for u-quarks, d-quarks, $\bar{u}$-quarks, $\bar{d}$-quarks and s-quarks (from top to bottom). The hatched areas represent the systematic uncertainties of the data.

panel of fig. 1. The most recent HERMES measurements focussed on the structure function $g_1^d(x)$. In the middle panel of fig. 1 the corresponding results are shown, which are based on data collected in the years 1998 through 2000 using a longitudinally polarized deuterium target. The results are seen to agree with those obtained at SLAC [4,7] and CERN [6], but have an improved precision.

The data shown in the bottom panel of fig. 1 have been obtained on a polarized ^{3}He target [8–10]. These data confirm the general conclusion that can be derived from fig. 1, *i.e.* that all presently available data are in good agreement which each other for each target. Improvements of the data are mainly needed at very low values of x (below 0.004) and very high values of x (above 0.6).

2.2 Flavour decomposition

Semi-inclusive deep-inelastic scattering experiments that make use of both polarized lepton beams and polarized targets in principle enable the determination of the polarized quark distributions $\Delta q_f(x)$ for each flavour f. From the experimental data the double spin-asymmetries $A_1^h(x)$ are extracted for different hadron types h. The asymmetries $A_1^h(x)$ are related to the quark distributions $\Delta q_f(x)$ through the so-called purity matrix p_f^h, which describes the probability that a hadron h originates from a quark of flavour f. The values of the matrix elements p_f^h are determined from Monte Carlo simulations based on the Lund string fragmentation model. Using this technique the HERMES Collaboration has obtained values for $x\Delta u$, $x\Delta d$, $x\Delta\bar{u}$, $x\Delta\bar{d}$, and $x\Delta s$, which are shown in fig. 2. In the analysis a s-$\bar{s}$ symmetric strange quark polarisation is assumed, and the data were evolved to a common Q^2 value of 2.5 GeV^2. As compared to previous data of this kind [2,3], the accuracy of the data on Δu and Δd has improved considerably, while it is the first time that separate spin distributions for the three sea-quark flavours have been obtained.

From the data shown in fig. 2 it is concluded that the u-quarks are strongly polarized in a direction parallel to that of the proton spin, while the d-quarks are weakly polarized in the opposite direction. The u and d sea quarks are seen to carry a small amount of spin, while there is a hint for a small positive s-quark polarization at low x (where the systematic uncertainty is largest).

The data are compared to two parameterisations of particle distribution functions, which are based on inclusive data only. The dashed line represents the GRSV parameterisation [11] using the so-called "standard scenario" in leading order. The dashed-dotted line represents the result of a leading order QCD parameterisation due to Bluemlein and Boettcher [12]. In all cases a reasonable to good description of the data is obtained.

3 Generalized parton distributions

Generalized parton distributions (GPDs) represent a new theoretical development, which encompasses both the well-known parton distribution functions (PDFs) and the nucleon form factors as limiting cases. While the PDFs describe the probability to find a parton with fractional momentum x in the nucleon (forward scattering), the GPDs describe the interference between quarks with momentum fractions $x+\xi$ and $x-\xi$ in the nucleon (off-forward scattering). Hence, the GPDs are sensitive to partonic correlations.

In 1997 Ji [13] has shown that the first moment of certain GPDs, which are accessible in deeply virtual Compton scattering (DVCS), are related to the total angular momentum of the quarks and the gluons in the nucleon. Experimentally one has to distinguish the DVCS process from the Bethe-Heitler (BH) process, which is usually largely dominant in an electron scattering environment. However, by exploiting the interference between the DVCS and BH processes, it is possible to obtain access to the DVCS amplitude [14]. As the interference term in the cross-section depends on the polarization and charge of the beam, and the azimuthal angle ϕ of the emitted photon (about the direction of the virtual photon), measurements of the ϕ-dependence of the beam-spin and beam-charge asymmetry are needed.

3.1 Beam-spin asymmetry in DVCS

The beam-spin asymmetry in hard electroproduction of photons has been measured both by the HERMES experiment at DESY [15] and the CLAS experiment at JLab [16]. In both cases an asymmetry with respect to the helicity state of the incoming lepton beam is observed if the missing energy is chosen to be close to the proton mass. The observed asymmetry has a clear $\sin\phi$ dependence, as expected from the DVCS-BH interference.

Since the first results were published, additional DVCS analyses have been carried out by the HERMES Collaboration. In fig. 3 the beam-spin asymmetry is shown as a function of ϕ for data collected in 2000. The previous observations (which were based on data collected in 1997) are confirmed with improved statistics. Moreover, the beam-spin analyzing power $A_{LU}^{\sin\phi} = \frac{2}{N}\sum_{i=1}^{N}\frac{\sin\phi_i}{(P_l)_i}$ with $(P_l)_i$ the beam polarization measured during the beam burst of the i-th event, has been evaluated. The quantity $A_{LU}^{\sin\phi}$ corresponds to the amplitude of the $\sin\phi$-fit of the single spin asymmetry. The data do not reveal any strong x, t or Q^2 dependence of $A_{LU}^{\sin\phi}$, but unfortunately the available statistics do not allow to make a 3-dimensional binning in these 3 variables. As there can be compensating kinematic dependences, considerably more data are needed before more definite conclusions can be drawn.

3.2 Beam-charge asymmetry in DVCS

While the beam-spin asymmetries give information on the imaginary part of the DVCS-BH interference amplitudes,

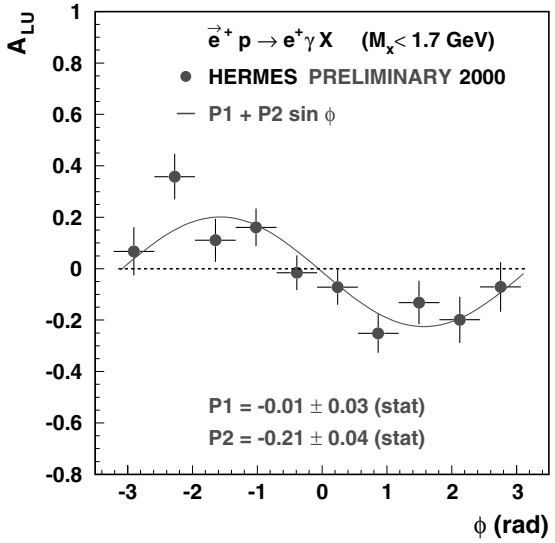

Fig. 3. Single beam-spin asymmetry for electroproduction of real photons on an unpolarized hydrogen target as a function of the azimuthal angle ϕ. The curve represents a $\sin\phi$-fit to the data, of which the amplitude ($P2$) and offset ($P1$) are shown.

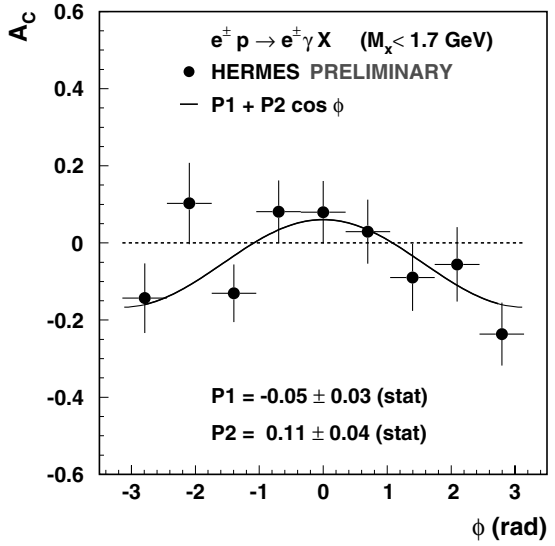

Fig. 4. Single beam-charge asymmetry for electroproduction of real photons on an unpolarized hydrogen target as a function of the azimuthal angle ϕ. The curve represents a $\cos\phi$-fit to the data, of which the amplitude ($P2$) and offset ($P1$) are shown.

the beam-charge asymmetry is sensitive to the real part of these amplitudes. A measurement of the beam-charge asymmetry requires the availability of both electron and positron beams at the same experimental set-up; both beams are available at HERA.

In fig. 4 the first measurements of the single beam-charge asymmetry for electroproduction of real photons on an unpolarized hydrogen target are shown. The data have low statistics, but show evidence of the expected $\cos\phi$ dependence [14]. If the $\cos\phi$-moment of the data is evaluated non-zero values are only seen in the "exclusive" region around $M_x \approx m_{\mathrm{proton}}$.

The new DVCS data demonstrate the feasibility of studying Compton scattering at the partonic level. It is also clear that the statistics (and kinematic coverage) of such measurements has to be dramatically improved before DVCS data can be used to extract information on the total angular momentum carried by quarks.

4 Quark nuclear physics

The nuclear medium represents an additional degree of freedom in our efforts to study nucleon structure. In inclusive deep-inelastic lepton scattering, for instance, the A-dependence of the unpolarized structure function $F_2(x)$ may provide information on a possible density or nucleon momentum dependence of the quark distributions. In a similar vein it has been investigated whether the ratio of the longitudinal to transverse photon absorption cross-sections $R(x, Q^2)$ is A-dependent. A careful analysis of new ^{84}Kr data (and a reanalysis of existing ^{14}N data) has provided no conclusive evidence supporting such an A-dependence[1].

If additional hadrons are observed in deep-inelastic scattering on nuclear targets a possible momentum dependence of $F_2(x)$ can be studied (subsect. 4.1) and parton energy loss mechanisms can be investigated (subsect. 4.2).

4.1 Tagged structure functions

In order to study the feasability of observing (relatively slow) recoil protons in deep-inelastic lepton scattering a small Silicon Test Counter (STC) was built and installed just below the internal target of the HERMES experiment [19,20]. The STC was successfully operated for several months with unpolarized ^{1}H and ^{2}H targets. As the instrument was installed *inside* the vacuum of the HERA storage ring, and the HERMES internal target has a very thin cell wall ($\approx 75\,\mu$m), recoil protons with momenta down to 100 MeV/c could be observed.

While the primary physics purpose of recoil detection in deep-inelastic scattering is the identification of exclusive processes such as DVCS (see sect. 3), the low momentum threshold of the STC makes it also possible to study tagged structure functions. In fact, data collected at HERMES during the few months in which the STC was tested are sufficient for a first study of this subject.

When a slow recoil proton is observed in DIS on ^{2}H it can either be due to target fragmentation or it is a spectator proton that can be used as a tag of a DIS event on a neutron. The latter type of events can be isolated by subtracting recoil data collected on a ^{1}H target from the ^{2}H data properly weighted by the corresponding integrated luminosities. If the resulting recoil momentum spectrum is subsequently corrected for acceptance effects and kinematics, the nucleon momentum distribution $n(p)$ in ^{2}H can be derived from the data under the assumption that the integral (over x and Q^2) of the tagged and untagged structure functions are roughly the same. The derived values of $n(p)$ are displayed in fig. 5. Within the relatively large systematic uncertainties (of about 16%), the data are seen to be in surprisingly good agreement with both a relativistic plane-wave calculation of Tjon [21], and a parameterisation of existing data obtained in *quasi-elastic* kinematics [22].

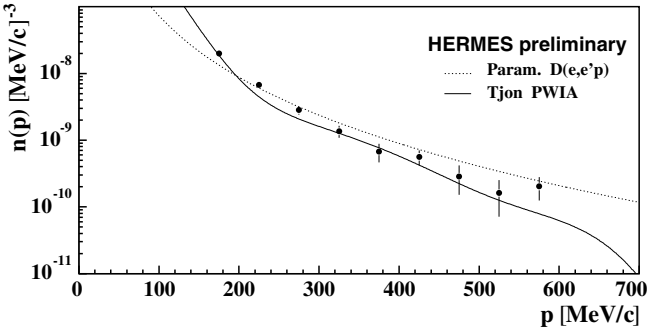

Fig. 5. Momentum distribution of spectator protons observed in deep-inelastic scattering off ^{2}H. Fragmentation products are subtracted using data collected on ^{1}H. The dotted curve corresponds to a parameterisation of ^{2}H$(e, e'p)$ data obtained in quasi-elastic kinematics [23], while the solid curve represents a calculation of the plane-wave momentum distribution of the nucleons in ^{2}H [21].

It is concluded that the spectator mechanism is at work in deep-inelastic scattering, and can thus be used to tag structure functions. Consequently, high-statistics data of this kind will enable a study of the nucleon momentum dependence of $F_2(x, Q^2)$. Such a momentum dependence of $F_2(x, Q^2)$ has been proposed as a possible explanation of the EMC effect [24]. Furthermore, the success of the spectator model implies that the nucleon momentum distribution in ^{2}H can —in principle— be measured as well in deep-inelastic scattering. Usually, the momentum distribution $n(p)$ is determined in quasi-elastic knock-out experiments. However, such measurements are known to be hampered by relatively large meson-exchange and $\Delta(1232)$ contributions [23] —in particular at high p, neither of which contribute in deep-inelastic scattering. On the other hand, a proper treatment of the final-state interaction between the fragmentation products and the spectator proton will require further theoretical study.

4.2 Quark propagation in nuclei

In a recent paper Wang [25] calculated the energy loss of propagating partons in hot or cold nuclear matter. The effect of parton rescattering and energy loss is cast in an effective modification of the fragmentation function, $D_{\rm eff}(z) \approx \frac{1}{1-\Delta E/E} D(\frac{z}{1-\Delta E/E})$ with ΔE the average partonic energy loss. By comparing this type of calculation to results obtained from semi-inclusive deep-inelastic scattering data collected by the HERMES Collaboration on ^{14}N and ^{84}Kr, a value for ΔE in cold nuclear matter is obtained. The resulting calculation of $D_{\rm eff}/D$ is compared to the data in fig. 6. In this figure the ratio of

[1] The previously reported [17] A-dependence of R turned out to be due to an artefact of the analysis [18].

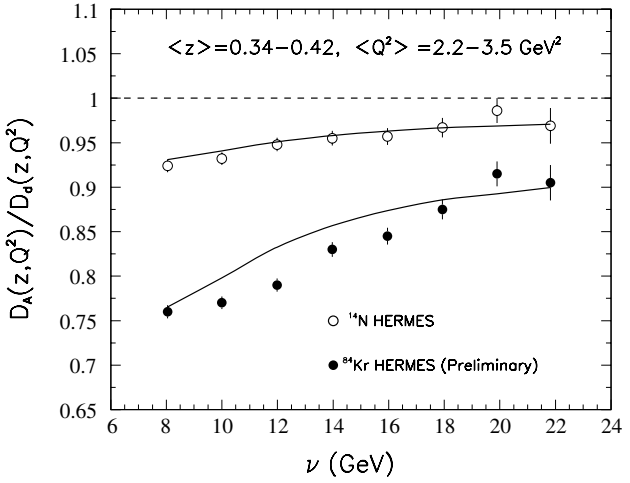

Fig. 6. Multiplicity ratio of hadrons produced on ^{14}N (open circles) and ^{84}Kr (solid circles) normalized to the multiplicity ratio as obtained on ^{2}H. (This superratio is expressed as a ratio of fragmentation functions [1].) The curves are from ref. [1] in which the parton energy-loss was adjusted to 0.3 GeV/fm.

the hadron yields per DIS event on ^{14}N (and ^{84}Kr) to the same yield as obtained on deuterium is plotted *versus* the energy transfer ν. The data show a significant (energy-dependent) attenuation, which is larger for ^{84}Kr than for ^{14}N. This hadron attenuation is well described by the aforementioned calculations of Wang if an energy loss per unit of distance of about 0.3 GeV/fm is taken.

This value for the partonic energy loss in cold nuclear matter can be compared to the energy loss derived from recent PHENIX data [26] on π^0 production in Au + Au collisions at $\sqrt{s} = 130$ GeV, yielding 0.25 GeV/fm [25]. If the PHENIX number is converted to the corresponding energy loss in the initial hot stage of the Au + Au collision, a value of about 4.5 GeV/fm is found. Comparing this number to the value derived from the HERMES data for cold nuclear matter, it is concluded that the gluon density (which drives the energy loss) is a factor 15 higher in the initial phase of the Au + Au collision. This result reflects an interesting link between two fields that used to be essentially independent: relativistic heavy-ion collisions, and deep-inelastic scattering.

5 Outlook

Experiments studying the structure of the nucleon have expanded considerably beyond the well-known inclusive deep-inelastic lepton scattering experiments, which —by now— have yielded precise data on the unpolarized structure function $F_2(x)$ and the spin-dependent structure function $g_1(x)$. As an example of these developments the new data on the flavour decomposed quark spin distributions were presented, showing that the sea quarks carry only little spin angular momentum. Another example is offered by data on deeply virtual Compton scattering, which —if pursued at higher luminosity— may give information on the *total* angular momentum carried by the partons.

Several new results have also been obtained with unpolarized experiments on heavy nuclei, the true domain of *quark nuclear physics*. The first measurement of the momentum spectrum of recoil protons in deep-inelastic scattering on ^{2}H demonstrated the validity of the spectator model, which will enable the study of the p-dependence of $F_2(x)$ in the future. The attenuation of hadrons produced in semi-inclusive experiments provided a value for the parton energy loss in cold nuclear matter, which is of great relevance as a benchmark for the interpretation of relativistic heavy-ion collisions.

These developments, which in several cases represent only first low-statistics measurements demonstrating the feasability of a new technique, call for the construction of new high-luminosity deep-inelastic lepton scattering facilities. Both in Europe and the US such plans are being actively discussed [27].

I would like to thank all my collegues from the HERMES Collaboration for making it possible to perform an experiment that has produced so many high-quality data. Ed Kinney and Dirk Ryckbosch are kindly acknowledged for carefully reading the manuscript.

References

1. X. Guo, X.N. Wang, Phys. Rev. Lett. **85**, 3591 (2000).
2. B. Adeva *et al.*, Phys. Lett. B **420**, 180 (1998).
3. K. Ackerstaff *et al.*, Phys. Lett. B **464**, 123 (1999).
4. P.L. Anthony *et al.*, Phys. Lett. B **463**, 339 (1999); Phys. Lett. B **493**, 19 (1999).
5. A. Airapetian *et al.*, Phys. Lett. B **442**, 484 (1998).
6. B. Adeva *et al.*, Phys. Rev. D **58**, 112001 (1998); Phys. Rev. D **60**, 072004 (1999).
7. K. Abe *et al.*, Phys. Rev. Lett. **76**, 587 (1996); Phys. Rev. D **58**, 112003 (1998).
8. P.L. Anthony *et al.*, Phys. Rev. Lett. **71**, 959 (1993); Phys. Rev. D **54**, 6620 (1996).
9. K. Abe *et al.*, Phys. Rev. Lett. **79**, 26 (1997).
10. K. Ackerstaff *et al.*, Phys. Lett. B **404**, 383 (1997).
11. M. Glück, E. Reya, M. Stratmann, W. Vogelsang, Phys. Rev. D **63**, 094005 (2001).
12. J. Blumlein, H. Boettcher, hep-ph/0203155 (scen. 1).
13. X. Ji, Phys. Rev. D **55**, 7114 (1997).
14. M. Diehl *et al.*, Phys. Lett. B **411**, 193 (1997).
15. A. Airapetian *et al.*, Phys. Rev. Lett. **87**, 182001 (2001).
16. S. Stepanyan *et al.*, Phys. Rev. Lett. **87**, 182002 (2001).
17. K. Ackerstaff *et al.*, Phys. Lett. B **475**, 386 (2000).
18. A. Airapetian *et al.*, submitted to Phys. Lett. B (2002).
19. K.T. Fiedler, PhD Thesis, University of Nürnberg-Erlangen, 2001.
20. J. Visser, PhD Thesis, University of Groningen, 2002.
21. E. Hummel, J. Tjon, Phys. Rev. C **49**, 21 (1994), and private communication.
22. F. Krautschneider, PhD Thesis, University of Bonn, 1976.
23. W.-J. Kasdorp *et al.*, Few-Body Systems **25**, 115 (1998).
24. J. Ashman *et al.*, Phys. Lett. B **206**, 364 (1988).
25. X.N. Wang, hep-ph/0111404; E. Wang, X.N. Wang, hep-ph/0202105.
26. K. Adcox *et al.*, Phys. Rev. Lett. **88**, 022301 (2002).
27. G. van der Steenhoven, *Concluding remarks on QCD-N'02 Workshop in Ferrara*, Nucl. Phys. A **711**, 363c (2002).